ChemComm

Iron Polypyridyl Complex Adsorbed on Carbon Surfaces for Hydrogen Generation

Journal:	*ChemComm*
Manuscript ID	CC-COM-04-2021-002131.R1
Article Type:	Communication

COMMUNICATION

Iron Polypyridyl Complex Adsorbed on Carbon Surfaces for Hydrogen Generation†

Received 00th January 20xx,
Accepted 00th January 20xx

DOI: 10.1039/x0xx00000x

Caroline M. Margonis, Marissa Ho, Benjamin D. Travis, William W. Brennessel‡, and William R. McNamara*

A series of homogeneous Fe(III) complexes were recently reported that are active for electrocatalytic hydrogen generation. Herein we report a napthalene-terminated Fe(III) complex for use in the functionalization of glassy carbon surfaces for electrocatalytic hydrogen generation with retention of catalytic activity.

Through artificial photosynthesis (AP), solar energy can be harvested and used to split water into H_2 and O_2.[1] The reductive side of AP focuses on the conversion of protons to hydrogen gas.[1] Many transition metal complexes have been demonstrated to be active electrocatalysts for hydrogen generation.[2] However, development of systems integrating inexpensive materials is essential for wide-spread applications.[3] As the most Earth-abundant metal, iron is widely accessible and relatively low in cost, which makes incorporation of iron into large-scale AP systems more economically feasible.

To this end, we have recently reported a series of iron polypyridyl monophenolate complexes that are active for electrocatalytic hydrogen generation (Fig. 1).[4] Electrocatalysis by complex **1** occurs at -1.57 V vs. Fc^+/Fc in CH_3CN with a turnover frequency up to 1000 s^{-1} and a 660 mV overpotential.[4] Catalytic activity is enhanced in the presence of water, with **1** achieving turnover frequencies of 3000 s^{-1} and operating with an 800 mV overpotential.[4] The complex is also is active for photocatalysis when paired with fluorescein (chromophore) and triethylamine (sacrificial donor) in 1:1 ethanol:water mixtures.[5] This highly active and stable system achieves TONs with respect to catalyst of >2100 after 24 hours of irradiation.[5] A second addition of the sacrificial donor after 24 hours restored hydrogen production activity.[5] The robustness of this system is further highlighted catalytic activity achieved in solutions containing local pond water.[5]

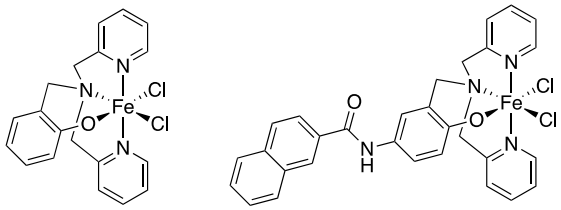

Fig. 1 Left: Iron polypyridyl monophenolate parent catalyst (**1**). Right: Naphthalene-terminated iron polypyridyl monophenolate parent catalyst (**2**).

Although highly active, hydrogen evolution by homogeneous systems is limited by diffusion.[6] A promising method to overcome this issue and expedite the electron-transfer process is to anchor the catalyst to a wide band gap semiconductor, such as TiO_2, or $SrTiO_2$.[6] However, fast photo-generated electron-hole pair recombination before participation in the redox reaction can limit the activity of these systems.[7] Therefore, it is critical to examine a wide range of semiconductor surfaces. Carbon nanotubes (CNTs) have shown great promise as a semiconductor support for hydrogen generation catalysts.[8] Several of such systems incorporating a CNT-enhanced semiconductor and a Pt-loaded catalyst have also been found to be active for photocatalytic hydrogen generation.[9]

College of William and Mary, 540 Landrum Drive, Williamsburg, VA 23185, USA. Email: wrmcnamara@wm.edu
‡University of Rochester, 252 Elmwood Ave, Rochester, NY 14611
†Electronic Supplementary Information (ESI) available: Crystallographic information files and experimental details. See DOI: 10.1039/x0xx00000x

One method of immobilizing iron catalysts on CNT surfaces involves adsorption to the surface through π-π stacking interactions.[10] As a non-covalent interaction, these forces are typically much weaker than covalent bonds, but the magnitude of attraction can be modified by altering the size of the pi-stacking network; calculations on the strengths of π-π-stacking interactions between aromatic molecules and CNTs suggest that binding energies are in the range of 10-25 kJ/mol per benzene ring, signifying that the strength of the attachment increases with the size of the polyaromatic network.[11] Furthermore, adsorption of π-π stacking molecules is reversible, suggesting that the structure of the catalyst may remain intact.

In order to develop an iron polypyridyl monophenolate catalyst capable of adsorption to carbon surfaces, a ligand was designed that contains both the polypyridyl ligand and a pendant naphthalene group (Fig. 1). The naphthalene group was selected based on its previously demonstrated capacities for carbon surface adsorption and functionalization.[10] The naphthalene-terminated ligand was synthesized and subsequently coordinated to $FeCl_3$ to give **2**, and crystals suitable for X-ray diffraction were grown through the slow diffusion of toluene into a concentrated solution of **2** in dichloromethane.

The complex presents itself as a disoriented octahedral, with the Fe(III) centre bound to two chlorides and the ligand (Fig. 2). Distortion is evident based on deviation from the expected octahedral-bond angles, which likely occurs to minimize strain arising from the 6-membered chelate ring, resulting from coordination of the phenolate and N(3) to the iron centre. Additionally, disorder within the crystal arises from a planar flip of the naphthalenyl group, which is modelled as being disordered over two positions (0.80:0.20); because the two orientations do not fill the exact same relative special volume, the co-crystallized solvent is disorganized to accommodate them (see ESI†).

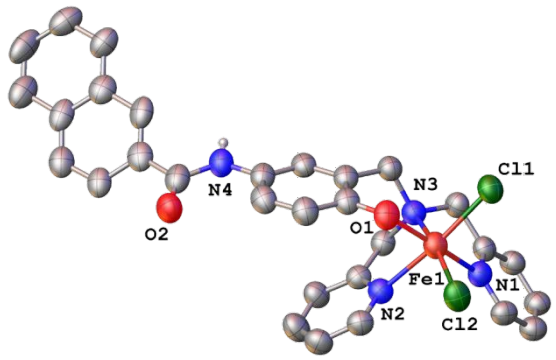

Fig. 2 ORTEP diagram of **2** with Fe (orange), O (red), N (blue), Cl (green), and C (gray). Hydrogen atoms are omitted for clarity.

Cyclic voltammetry was used to observe and characterize the adsorption behaviour of **2** on the surface of glassy carbon electrodes. Though not as large or pristine as the graphene surfaces found in CNTs, the smaller domains of sp^2 hybridized carbon in glassy carbon allow this electrode to act as a convenient model system.[12] Electrodes were soaked overnight

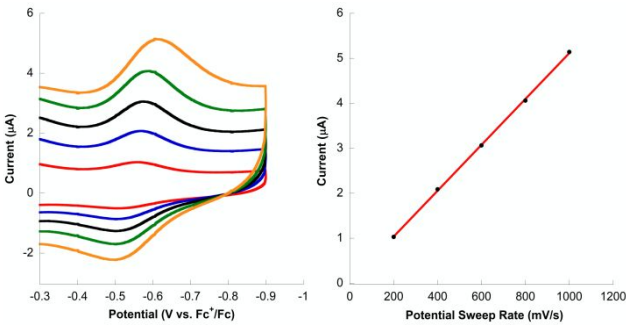

Fig. 3 Left: Cyclic voltammograms of **2** adsorbed to the surface of a glassy carbon electrode in 5 mL of 0.1 M $TBAPF_6$ in CH_3CN taken at scan rates of 200 (red), 400 (blue), 600 (black), 800 (green), and 1000 (orange) mV/s. Right: Cathodic peak current versus potential sweep rate for **2** (R^2 = 0.99972).

in a 0.5 mM solution of **2** before being removed, rinsed with CH_3CN, and added to an electrochemical cell containing 0.1 M $TBAPF_6$ in CH_3CN. The working electrode was cycled between +0.2 and -0.95 V vs Fc^+/Fc to observe only the Fc^+/Fc (internal standard) and Fe(III)/Fe(II) redox couples and to minimize the possibility of reductive desorption.

Cyclic voltammograms of surface-adsorbed **2** taken at various potential scan rates show a reversible Fe(III)/Fe(II) reduction at -0.60 V vs Fc^+/Fc. This potential is 100 mV more positive than the homogeneous parent complex **1** (Fig. 4). For an electroactive adsorbate, the peak current increases linearly with the potential sweep rate.[13] This contrasts the redox behaviour of a freely-diffusing material, in which there is a linear relationship between the peak current and the square root of the scan rate.[13] The linearity (R^2 > 0.99) of the peak current versus potential scan rate plot for **2** indicates that the observed electrochemical response arises from material adsorbed onto the surface of the glassy carbon electrode rather than from material freely diffusing in solution (Fig. 3). Quantitatively, the relationship between peak current and potential scan rate for an electroactive adsorbate is given to be:[13]

$$i_p = \frac{n^2F^2}{4RT}\upsilon A\Gamma^*$$

where i_p is the peak current, n is the number of electrons transferred in the redox event, F is the Faraday constant, R is the gas constant, T is the temperature, υ is the potential sweep rate, A is the surface area of the electrode, and Γ^* is the surface coverage of the adsorbed species.[13] As such, the relationship between peak current and potential sweep rate can be used to calculate the surface coverage of **2**, which was found to have a value of 7.7 x 10^{-11} mol/cm^2 at 298 K. This value is similar to a previously reported naphthalene-terminated cobalt complex.[10]

Another expected characteristic of an electroactive adsorbate is a separation less than 58 mV between the peak of the anodic wave and the peak of the cathodic wave (ΔE_p).[13] This behaviour is observed for the 200 and 400 mV/s scans, in which ΔE_p is 42 and 43 mV respectively, of **2**. However, ΔE_p continues to increase with the scan rate and reaches upwards of 104 mV

with a potential sweep rate of 1000 mV/s. This deviation from the ideal behaviour indicates that a kinetic barrier to electron transfer exists. Despite these variations, ΔE_p for the naphthalene complex is still significantly less than the homogeneous complex, **1,** at all potential scan rates (Fig. 4). The smaller ΔE_p of **2** compared to **1** indicates that **2** is adsorbed to the electrode surface and is not freely diffusing in solution.

To confirm that the adsorption behaviour observed was a specific result of pi-stacking interactions between the naphthalene moiety and the electrode surface, analogous iron complexes with different functional groups were examined. These complexes have the same basic structure, but lack the naphthalene anchoring group. Following the same overnight electrode soaking procedure, no electrochemical response was observed using electrodes soaked overnight in individual solutions of these complexes (see ESI†). This indicates that the naphthalene moiety plays a critical role in surface adsorption.

Following confirmation of adsorption behaviour, the adsorption kinetics of **2** were examined by soaking the glassy carbon electrode in a 0.5 mM solution of **2**, rinsing, and collecting CVs. The measured current, which is linearly related to the surface coverage of the catalyst, initially grows with soak time. The most rapid growth is seen within the first 60 minutes, in which the cathodic peak current reaches 83% of its maximum value. The current peaks at a soak time of 720 minutes, which marks the point at which the adsorbed material is at equilibrium with the freely diffusing material in the solution (see ESI†).

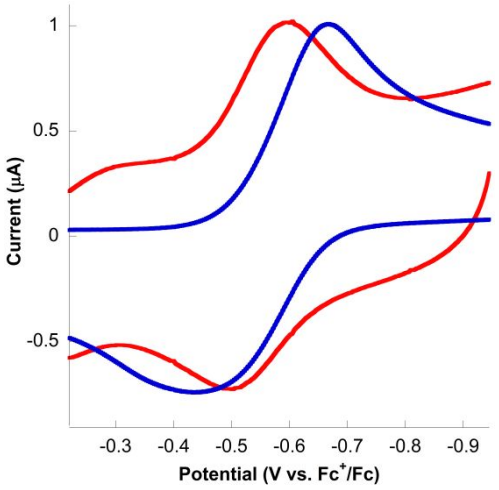

Fig. 4 Cyclic voltammograms of **2** (red) adsorbed to the surface of a glassy carbon electrode and 0.1 mg of **1** (blue) in 5 mL of 0.1 M $TBAPF_6$ in CH_3CN taken at 200 mV/s.

With adsorption behaviour characterized, its ability to function as an electrocatalyst for proton reduction was examined. CVs of the electrode-adsorbed catalyst were obtained upon the addition of known concentrations of trifluoroacetic acid (TFA) in acetonitrile. In the presence of TFA, an irreversible reduction event is observed at -1.53 V vs. Fc^+/Fc (Fig. 5). At the same [TFA], this catalytic wave for **2** occurs at a potential 120 mV more positive than that of **1**. The peak current of this proton reduction wave increases linearly with [TFA], suggesting a second order dependence on [H^+], which is consistent with what is observed for **1** (see ESI†). Upon addition of a proton source, the Fe(III)/Fe(II) redox couple shifts 340 mV to a more anodic potential. This behavior is consistent with what is observed for the homogeneous catalyst, **1**. The positive shift of the Fe(III)/Fe(II) redox couple suggests that the first step

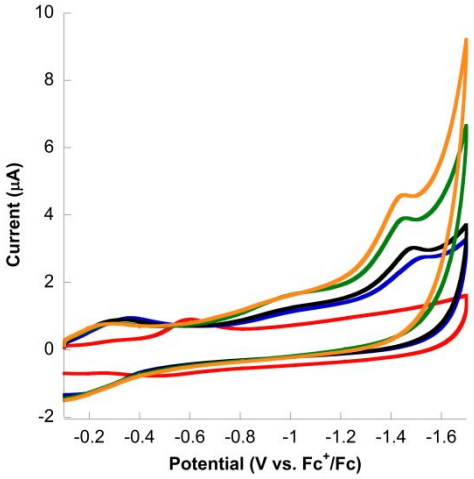

Fig. 5 Cyclic voltammograms of surface adsorbed **2** in 5 mL of 0.1 M $TBAPF_6$ in CH_3CN in the presence of no acid (red), 0.4 mM (blue), 0.8 mM (black), 1.2 mM (green), and 1.6 mM (orange) at 200 mV/s**.**

in the mechanism is a chemical step (C), or more specifically, the protonation of the phenol group. The complex then undergoes electron transfer, (E), to be reduced to Fe(II). The subsequent increase in current observed at -1.53 V corresponds to another reduction and protonation event to liberate hydrogen gas. This suggests a CECE or CEEC mechanism, similar to what is observed for **1**. Furthermore, when a potential of -1.6 V vs Fc^+/Fc is applied in a bulk electrolysis experiment, hydrogen evolution is observed with a faradaic yield of 99% (see ESI†). With an i_c/i_p = 5.46, complex **2** exhibits similar activity to **1** (see ESI†), but with an overpotential of 480 mV compared to 660 mV for **1** (see ESI†).".

In addition to TFA, tosic acid was examined as a proton source for hydrogen generation catalyzed by **2**. In the presence of 0.4 mM tosic acid, an irreversible catalytic wave corresponding to proton reduction is observed at -1.43 V vs.

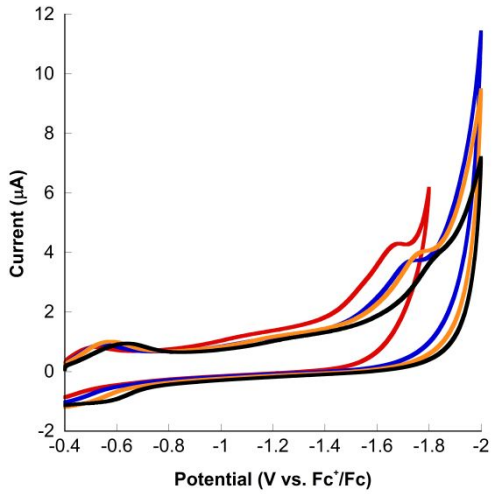

Fig. 6 Cyclic voltammograms of surface adsorbed **2** in 5 mL of citrate-buffered aqueous solutions at pH 3.8 (red), 4.6 (blue), 5.4 (orange) and 6.2 (black).

Fc^+/Fc (see ESI†). However, in contrast to the TFA additions, the current of the proton reduction peak decreases with increasing tosic acid concentrations. This decrease in current can be attributed to desorption of **2** from the electrode surface at higher acid concentrations.

Since an ideal catalyst for AP is active in aqueous solutions, the catalytic activity of **2** was examined in aqueous buffer solutions. Catalytic reduction waves were observed for each pH. A 52 and 64 mV variation in Fe(III)/Fe(II) redox couple is observed per pH unit (see ESI†).

In summary, we have synthesized a naphthalene-terminated iron polypyridyl monophenolate complex capable of adsorbing to glassy carbon electrodes. Additionally, this complex is electrocatalytically active for proton reduction in the presence of TFA with catalysis occurring at -1.53 V vs. Fc^+/Fc and operating with an overpotential of 480 mV. The catalyst is also active in purely aqueous buffer solutions of pH = 3.8 – 6.2. This result underscores the versatility of using π-staking interactions to immobilize proton reduction catalysts on sp^2-hybridized carbon surfaces.

We are grateful to the National Science Foundation (CHE-1749800) for funding. WRM also thanks the Henry Dreyfus Foundation for funding.

Conflicts of interest

There are no conflicts to declare.

Notes and references

1 (a) D. G. Nocera, *Acc. Chem. Res*., 2012, **45**, 767–776; (b) N. S. Lewis and D. G. Nocera, *Proc. Natl. Acad. Sci. U. S. A*., 2006, **103**, 15729; (c) R. Eisenberg, *Science*, 2009, **324**, 44; (d) J. L. Dempsey, B. S. Brunschwig, J. R. Winkler and H. B. Gray, *Acc. Chem. Res*., 2009, **42**, 1995–2004; (e) D. Kim, K. K. Sakimoto, D. Hong and P. Yang, *Angew. Chem., Int. Ed.*, 2015, **54**, 3259–3266.

2 (a) P. Connolly and J. H. Espenson, *Inorg. Chem*., 1986, **25**, 2684; (b) X. Hu, B. S. Brunschwig and J. C. Peters, *J. Am. Chem. Soc*., 2007, **129**, 8988; (c) C. Baffert, V. Artero and M. Fontecave, *Inorg. Chem*., 2007, **46**, 1817; (d) P. A. Jacques, V. Artero, J. Pecaut and M. Fontecave, *Proc. Natl. Acad. Sci. U. S. A.*, 2009, **106**, 20627; (e)D. L. Du Bois, *Inorg. Chem*., 2014, **53**, 3935–3960; (f) R. M. Bullock, A. M. Appel and M. L. Helm, *Chem. Commun*., 2014, **50**, 3125–3143; (g) Y. Sun, J. P. Bigi, N. A. Piro, M. L. Tang, M. J. R. Long and C. J. Chang, *J. Am. Chem. Soc.*, 2011, **133**, 9212; (h) H. I. Karunadasa, C. J. Chang and J. R. Long, *Nature*, 2010, **464**, 1329–1333; (i) B. Stubbert, J. C. Peters andH. B. Gray, *J. Am. Chem. Soc*., 2011, **133**, 9212; (j) X. Zhao, I. P. Georgakaki, M. L. Miller, J. C. Yarbrough and M. Y. Darensbourg, *J. Am. Chem. Soc*., 2001, **123**, 9710–9711; (k) G. A. N. Felton, R. S. Glass, D. L. Lichtenberger and D. H. Evans, *Inorg. Chem*., 2006, **45**, 9181–9184; (l) M. E. Carroll, B. E. Barton, T. B. Rauchfuss and P. J. Carroll, *J. Am. Chem. Soc*., 2012, **134**, 18843–18852; (m) S. Kaur-Ghuman, L. Schwartz, R. Lomoth, W. Stein and S. Ott, *Angew. Chem., Int. Ed*., 2010, **49**, 8033; (n) A. D. Nguyen, M. D. Rail, M. Shanmugam, J. C. Fettinger and L. A. Berben, *Inorg. Chem*., 2013, **52**, 12847–12854.

3 (a) S. C. Eady, M. M. MacInnes and N. Lehnert, *Inorg. Chem*., 2017, **56**, 11654–11667; (b) R. J. DiRisio, J. E. Armstrong, M. A. Frank,W. R. Lake and W. R. McNamara, *Dalton Trans*., 2017, **46**, 10418–10425.

4 (a) C. L. Hartley, R. J. DiRisio, T. Y. Chang, W. Zhang and W. R. McNamara, *Polyhedron*, 2016, **114**, 133–137; (b) A. C. Cavell, C. L. Hartley, D. Liu, C. S. Tribble and W. R. McNamara, *Inorg. Chem*., 2015, **54**, 3325–3330; (c) G. P. Connor, K. J. Mayer, C. S. Tribble and W. R. McNamara, *Inorg. Chem*., 2014, **53**, 5408–5410.

5 C. L. Hartley, R. J. DiRisio, M. E. Screen, K. J. Mayer and W. R. McNamara, *Inorg. Chem*., 2016, **55**, 8865–8870.

6 N. A. Race, W. Zhang, M. E. Screen, B. A. Barden and W. R. McNamara, *Chem. Commun*., 2018, **54**, 3290–3293.

7 (a) C. D. Jaeger and A. J. Bard, *J. Phys. Chem*., 1979, **83**, 3146–3152. (b) X. Chen and S. Mao. *Chem Rev*. 2007, **107**, 2891–2959.

8 (a) Y. Yau, G. Li, S. Ciston, R. Lueptow and K. Gray, *Environ. Sci. Technol.,* 2008, **42**, 4952–4957. (b) I. Robel, B. A. Bunker and P. V. Kamat, *Adv. Mater*., 2005, **17**, 2458. (c) A. Le Goff, V. Artero, B. Jousselme, P. D. Tran, N. Guillet, R. Metaye, A. Fihri, S. Palacin, M. Fontecave, *Science,* **2009**, 326, 1384-1387.

9 Y. Kim and H. Park, *Energy Environ. Sci.*, 2011, **4**, 685–694. (b) K. Dai, T. Peng, D. Ke and B. Wei, *Nanotechnology*, 2009, **20**, 12.

10 H. L. Smith, R. L. Usala, E. W. McQueen and J. I. Goldsmith, *Langmuir*, 2010, **26**, 3342–3349.

11 T. Kar, H. F. Bettinger, S. Scheiner and A. K. Roy, *J. Phys. Chem.*, 2008, **112**, 20070–20075.

12 P. J. F. Harris. *Philos. Mag.*, 2004, **84**, 3159–3167.

13 (a) N. Elgrishi, K. Rountree, B. McCarthy, E. Rountree, T. Eisenhart and J. Dempsey. *J. Chem. Edu.*, 2018, **95**, 197–206. (b) A. J. Bard and L. R. Faulkner. *Electrochemical Methods,* 2nd ed, J. Wiley & Sons: New York, 2001.

